Dilepton production in nucleon-nucleon collisions reexamined

R. Shyam[1,2] and U. Mosel[3]
[1]*Saha Institute of Nuclear Physics, Kolkata 700064, India*
[2]*Theory Center, Thomas Jefferson National Accelerator Facility, 12000 Jefferson Avenue, Newport News, Virginia 23606, USA*
[3]*Institut für Theoretische Physik, Universität Giessen, D-35392 Giessen, Germany*
(Received 5 November 2008; published 10 March 2009)

We present a fully relativistic and gauge-invariant framework for calculating the cross sections of dilepton production in nucleon-nucleon (NN) collisions that is based on the meson-exchange approximation for the NN-scattering amplitudes. Predictions of our model are compared with those of other covariant models that have been used earlier to describe this reaction. Our results are also compared with those of the semiclassical models that are employed to get the input elementary cross sections in the transport model calculations of the dilepton production in nucleus-nucleus collisions. It is found that cross sections obtained within the semiclassical and quantum mechanical models differ noticeably from each other.

DOI: 10.1103/PhysRevC.79.035203 PACS number(s): 25.75.Dw, 13.30.Ce, 12.40.Yx

I. INTRODUCTION

A recurring feature of the dilepton (e^+e^-) spectra measured in nucleus-nucleus (AA) collisions has been the enhancement (above known sources) in the invariant mass distribution of the cross sections in the region of the vector meson (ρ^0 and ω) pole mass. This has been the case for experiments performed for bombarding energies ranging from as low as 1 GeV/nucleon (DLS data [1]), through the SPS energies (40–158 GeV/nucleon) [2–4] to the energies employed by the PHENIX Collaboration at Relativistic Heavy Ion Collider (which correspond to invariant mass of 200 GeV/nucleon) [5]. The enhancement seen at the SPS energies are understood in terms of the modification of the ρ-meson spectral function in the hadronic medium [6].

However, the large dileptons yields observed in the DLS experiment (in $^{12}C + {}^{12}C$ and $^{40}Ca + {}^{40}Ca$ collisions at 1–2 GeV/nucleon beam energies) in the invariant mass (M) range from 0.2 to 0.5 GeV are yet to be explained satisfactorily [7–11]. Independent transport model calculations have been unable to describe these data fully even after including contributions from (i) the decay of ρ and ω mesons that are produced directly from the nucleon-nucleon (NN) and pion-nucleon scattering in the early reaction phase [12], (ii) the in-medium ρ spectral functions [13], (iii) the dropping ρ mass with corresponding modification in the resonance properties [7], and (iv) an alternative scenario of the in-medium effect—a possible decoherence between the intermediate meson states in the vector resonance decay [10]. This led to calling this discrepancy a "DLS-puzzle" [7,12] that persists even now.

To resolve this unsatisfactory situation the high-acceptance dielectron spectrometer (HADES) has been built [11] that allows study of the dilepton production in elementary proton-proton (pp), proton-deuteron (pd), as well as in proton-nucleus (pA) and AA collisions with much wider acceptance region for beam energies up to 8 GeV/nucleon. Unlike the DLS experiment HADES also measures the dilepton yields in the quasifree proton-neutron (pn) scattering. The first set of data has already been published [11,14] by this group on $^{12}C + {}^{12}C$ collisions at beam energies of 1.0 and 2.0 GeV/nucleon. The remarkable fact is that these data agree well with those of the DLS Collaboration. Therefore, there is no longer any question against the validity of the DLS data and the previous failures to explain them by various transport models have to do with problems in the theoretical calculations.

On the theory side, in a recent HSD transport model calculation [15] it has been shown that if one uses larger cross sections for elementary pp and pn bremsstrahlung processes then the observed dilepton yields in the relevant invariant mass region for the $^{12}C + {}^{12}C$ collisions at 1–2 GeV/nucleon can be reproduced. The support for the enhanced elementary bremsstrahlung cross sections comes from the calculations of these processes presented in Ref. [16] within a model that is similar to that used in Ref. [17]. Although the calculations perfomed within the two models use the same input parameters yet the cross sections of Ref. [16] are larger than those of Ref. [17] by factors of 2–4. It has been further argued in Ref. [15] that elementary bremsstrahlung cross sections larger than those of Ref. [17] were reported in Ref. [18] within a similar type of model that employs, however, realistic T matrices to describe the initial NN collisions.

In this article, we examine the issue of the dilepton production in the elementary NN collisions to highlight and understand the differences seen in the predictions of various models [16–18] for the corresponding cross sections. This is important for a proper theoretical description of the new data on the dilepton production in elementary pp and pn collisions that are likely to be announced soon by the HADES Collaboration. This will also have vital implications for the predictions of the different transport models for the HADES dilepton yields in AA collisions. Indeed, in a very recent UrQMD transport model analysis of the HADES $C + C$ data [19], it has been shown that even without using the enhanced elementary bremsstrahlung cross sections of Ref. [16] the observed dilepton yields can be described fairly well at the 2.0 GeV/nucleon beam energy in the region of relevant M values. Although, this theory still underpredicts the data in this mass region at the 1.0 GeV/nucleon beam energy.

The major difference between models of Refs. [16–18] lies in the method of implementing the gauge invariance of the NN bremsstrahlung amplitudes. To investigate this issue, we

have recalculated the cross sections for the dilepton production in elementary pp and pn reactions within a fully relativistic and gauge-invariant model that is similar to that used in Refs. [16,17] [to be referred as full quantum mechanical model (FQM)] except for the fact that we have used a pseudoscalar (PS) nucleon-nucleon-pion ($NN\pi$) vertex instead of the pseudovector (PV) one employed by these authors. The reason is that with the PS coupling, the contact term (seagull diagram) is not involved in the total Lagrangian that, however, still remains gauge invariant for bare point like nucleons. With a PV $NN\pi$ coupling one needs to introduce a contact term to restore the gauge invariance of the total amplitude and different approaches [20] for constructing this contribution lead to very different results [21]. The use of the PS $NN\pi$ vertex makes our discussions free from this ambiguity.

In the computation of the amplitudes, strong form factors are introduced to quench the contributions from high momenta and to include effects due to the compositeness of the nucleon. However, this leads to the loss of gauge invariance. We show here that form factors at various vertices (hadronic as well as electromagnetic) can still be implemented in our model without loosing gauge invariance. We make a detailed comparison of the ingredients and predictions of FQM with those of the models of Refs. [16,18] and examine their validity critically. The predictions of the FQM is also compared with those of the semiclassical models that are used to obtain the elementary NN bremsstrahlung and delta isobar contributions to the elementary dilepton production reactions in transport models to calculate the cross sections for this reaction in AA collisions.

II. FORMALISM

A representative of the lowest-order Feynman diagrams contributing to the dilepton production within our model is shown in Fig. 1. The intermediate nucleon or resonances can radiate a virtual photon that decays into a dilepton [Figs. 1(a) and 1(b)]. There are also their exchange counterparts. In addition, there are diagrams of similar types where the virtual photon is emitted from the nucleon line on the right side. The internal meson line can also lead to dilepton emission [see Fig. 1(c)]. To evaluate various amplitudes, we

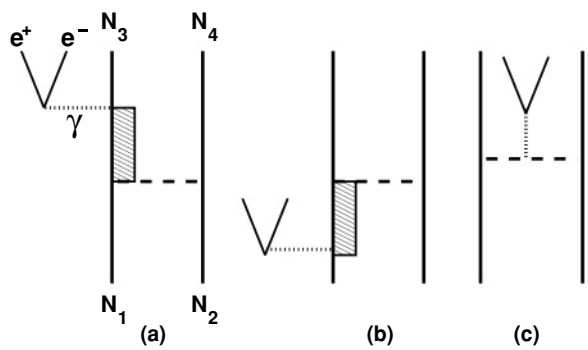

FIG. 1. A representative of Feynman diagrams for emission of dilepton in nucleon-nucleon collision as considered in this work. Emission (a) after NN collisions, (b) before NN collision, and (c) during NN collision. The box represents an off-shell nucleon or a Δ isobar.

have used the same effective Lagrangians for the nucleon-nucleon-meson, resonance-nucleon-meson, nucleon-nucleon-photon, and resonance-nucleon-photon vertices as discussed in Ref. [17] with the sole exception that for the $NN\pi$ vertex we have used the PS coupling

$$\mathcal{L}_{NN\pi} = ig_{NN\pi}\bar{\Psi}_N\gamma_5\tau\cdot\Phi_\pi\Psi_N \tag{1}$$

instead of the PV one. The parameters of the model were taken to be the same as those of Ref. [17] where details of calculations of various amplitudes are given. The on-shell equivalence of the pseudoscalar and pseudovector couplings makes the parameters independent of the choice for the type of the $NN\pi$ vertex.

In the computation of the amplitudes corresponding to diagrams shown in Fig. 1 the problem of loosing the gauge invariance arises while using the electromagnetic form factors if the complete vertex function for the half-off-shell photon production is not used [22–24]. The full vertex is given by

$$\Gamma^\mu(p',p) = e\sum_{i=1}^{3}\sum_{s,s'=\pm1}\Lambda^{s'}F_i^{s',s}(W',W;q^2)\mathcal{O}_i^\mu\Lambda^s(p), \tag{2}$$

where operators $\mathcal{O}$ are defined as $\mathcal{O}_1^\mu=\gamma^\mu$, $\mathcal{O}_2^\mu = -i\sigma^{\mu\nu}q_\nu/2m_N$, and $\mathcal{O}_3^\mu=-q^\mu$ with m_N being the nucleon mass. Λ's are projection operators that are given by

$$\Lambda^s(p) = \frac{s\gamma\cdot p + W}{2W}, \tag{3}$$

with $W=\sqrt{p^2}$ and $s=\pm1$. In Eq. (2) F_i are the form factors. In these equations p and p' denote the four momenta of the incoming and outgoing nucleons, respectively, and q is the four-momentum of the photon. We can relate F_1 and F_3 by using Ward-Takahashi identity (WTI) [22]

$$q_\mu\Gamma^\mu(p',p) = e\frac{(1+\tau_3)}{2}[S^{-1}(p') - S^{-1}(p)], \tag{4}$$

where $S(p)$ is the nucleon propagator. It should be noted that WTI does not pose any constraint on the magnetic form factor F_2.

It is easy to see that Eq. (4) will restore gauge invariance for the pn bremsstrahlung for the exchange of an uncharged meson (see, e.g., Ref. [22]). The current conservation condition (CCC) $q_\mu\Gamma^\mu=0$ is satisfied if the contributions of diagrams 1(a) and 1(b) are added together. In case of the exchange of charged mesons, however, the sum of these two diagrams does not vanish and one has to also include the contributions from the diagram 1(c) to fulfill the CCC.

In actual calculations the hadronic vertices also contain strong form factors that depend on the four momenta of the exchanged mesons. Therefore, for uncharged mesons, it is sufficient to multiply all the vertices by the same form factor as that of the hadronic vertices to keep the gauge invariance. However, the four-momentum of the meson changes in Fig. 1(c) for the case of the charged meson exchange and the corresponding meson current no longer satisfies the continuity equation even after being multiplied by the same hadronic form factor. One needs to multiply this form factor in diagram 1(c) [25] by an additional factor $F(\Lambda_\phi)$ that is obtained by letting $F(\Lambda_\phi)$ multiply the mesonic current and then solving

for the continuity equation. This leads to [26]

$$F(\Lambda_\phi) = 1 + \frac{m_\phi^2 - q_1^2}{\Lambda_\phi^2 - q_2^2} + \frac{m_\phi^2 - q_2^2}{\Lambda_\phi^2 - q_1^2}, \quad (5)$$

where Λ_ϕ is the cut-off parameter and q_1 and q_2 are the four-momentum transfers at the left and right vertices of graph 1(c), respectively. This result can be interpreted as the photon coupling to the regular pion (first term) and to "heavy" pion at the left and right vertices (second and third terms, respectively). This way of gauging the strong form factor makes it possible to use a given form factor for the meson and a different one for the nucleon but still fulfill the WTI.

As far as form factors for the electromagnetic vertices of the nucleons are concerned, we note that for real photons, the gauge invariance mandates $F_1 = 1, F_2 = \kappa_N$, and $F_3 = 0$, where κ_N is the magnetic moment of the nucleon. For the actual case there is a considerable uncertainty in these form factors. F_3 is never accessible by experiments because $\mathcal{O}_3^\mu j_\mu = 0$ for any conserved current. As in previous studies [16,17,22,27] we have chosen not to include electromagnetic form factors for the nucleon.

We now compare our model with those of Refs. [16,18]. In Ref. [18], instead of the one-boson exchange picture of our model, the nucleon-nucleon interaction is included via a T matrix that is based on the Paris potential. However, the nucleon current is not gauge invariant in this model. These authors rectify this problem in an ad hoc manner that may not have a microscopic basis. In the model of Ref. [16], a pseudovector $NN\pi$ coupling has been used. With this coupling gauge invariance is preserved with a contact term ($NN\pi\gamma$ vertex) added to the total Lagrangian. However, once hadronic form factors are introduced the gauge invariance will be violated and a gauge restoration procedure has to be applied [21].

In Ref. [16] the same method as described above has been used for restoring gauge invariance in the case of pp collisions. No contact graph due to pseudovector coupling appears in this case. For the np case, however, a contact term is needed. Different approaches for constructing the additional current contribution (contact term) to restore gauge invariance lead to different types of form factors [20] that can yield quite different results [21]. The usual practice is to choose a prescription that provides best agreement with the data. However, no comparison is shown with the experimental data in this article.

III. RESULTS AND DISCUSSIONS

In Fig. 2, we show the invariant mass distribution of the pp and pn bremsstrahlung contributions to the dilepton spectra at the beam energies of 1.04 and 2.09 GeV. Also shown here are results for this reaction as reported in Refs. [16,18]. First of all we remark that the cross sections calculated in the present work are very similar to those reported in our earlier work [17]—their shapes are unchanged while absolute magnitudes of the former are slightly larger than those of the latter (by about 10%). However, the cross sections reported for the pp case in Ref. [18] (to be referred as dJM) are larger than ours for invariant mass (M) < 0.25 GeV at the beam energy of 1.04 GeV while they are almost identical for 2.09 GeV in this mass region. At both the beam energies, dJM results are smaller than ours for $M > 0.25$ GeV. However, the cross sections of Ref. [16] (to be referred at KK) are larger than our results everywhere in the region of $M < 0.6$ GeV. An important point to note is that there is no overall multiplicative factor that differentiates the results of various models.

Despite using the same diagrams, input parameters and gauge invariance restoration procedure, our pp bremsstrahlung cross sections are lower than those of Ref. [16] as can be seen in the upper left panel of Fig. 2. Of course, in Ref. [16] a pseudovector $NN\pi$ vertex has been used as compared to the pseudoscalar one employed in this article. In this context, it is worthwhile to note that for the real photon production, the covariant model calculations do not depend on the choice of the $NN\pi$ coupling (PS or PV) as is shown in Ref. [28]. In case of dileptons, different results can arise for two couplings from the magnetic part of the $NN\gamma$ vertex. In fact, in Ref. [29] it is shown that pp dilepton bremsstrahlung contributions obtained with the PV $NN\pi$ coupling are actually smaller than those calculated with the PS one at the beam energy of 2 GeV. The calculations presented in Ref. [17] also support this to some extent. Because for the pn collisions, dJM results are not available, in the right panel of Fig. 2 we compare our results with KK cross sections only. We see that latter are larger than those of ours by factors ranging between 2 and 3 at both the beam energies.

In Fig. 3, we show a comparison of our results and those of Ref. [16] for the invariant mass distribution of the Δ isobar contribution to the dilepton production in pp and pn collisions at the beam energy of 1.04 GeV. We note that here too the KK cross sections are larger than ours by factors of $\sim$2 at smaller values of M even though the two models have used the same ingredients and input parameters for this part and there is no

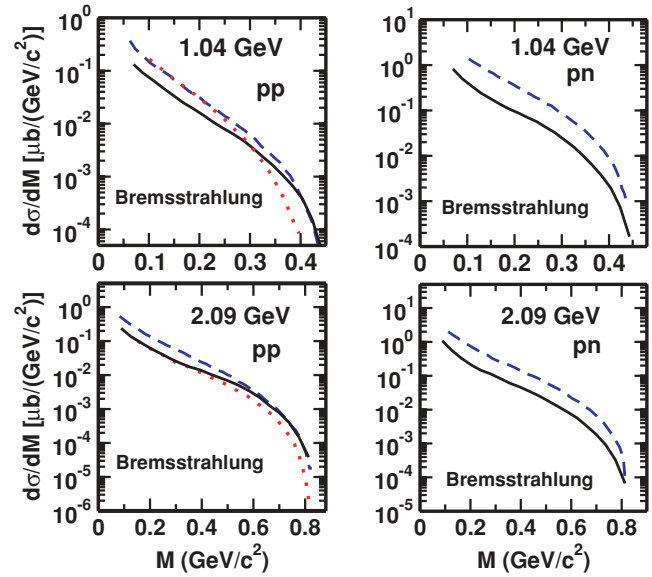

FIG. 2. (Color online) The invariant mass distribution of the NN bremsstrahlung contributions to the dilepton spectra in pp (left) and pn (right) collisions at the beam energies of 1.04 and 2.09 GeV. Results obtained within our model are shown by solid lines, whereas those of Refs. [18] and [16] by dotted and dashed lines, respectively.

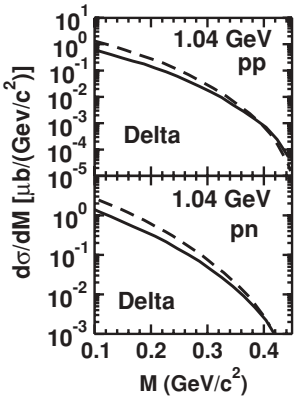

FIG. 3. The invariant mass distribution of the Δ isobar contribution to the dilepton spectra in *pp* (upper panel) and *pn* (lower panel) collisions at the beam energy of 1.04 GeV. The results of our model are shown by full lines while those of Ref. [16] by dashed line.

ambiguity related to gauge invariance as the resonance vertex is gauge invariant by its very construction.

In Fig. 4, we compare the total cross sections of the dilepton production in *pp* collisions with the DLS data at the beam energy of 1.04 GeV. The cross sections calculated within our model are folded with appropriate experimental filter and final mass resolution. The folded KK cross sections have been obtained by assuming that the folding procedure does not affect the ratios of the unfolded cross sections in the two cases. In this figure we have also shown cross sections for the π^0 Dalitz decay ($\pi^0 \to \gamma e^+ e^-$) that are the same as those shown in Ref. [17]. It is seen that KK cross sections overestimate the DLS data for $M < 0.3$ GeV where statistical errors are smaller. The data have larger error bars for $M > 0.3$ GeV. In this context the HADES data on the elementary dilepton production reactions are expected to be useful because of their low statistical error [30].

In the several transport model calculations of dilepton production in the *AA* collisions, the usual practice is to calculate the nucleon bremsstrahlung contributions within a soft photon approximation (SPA) model [31,32] and the delta contribution within a Dalitz decay (DDD) model [33]. The corresponding cross sections are added up to get the total

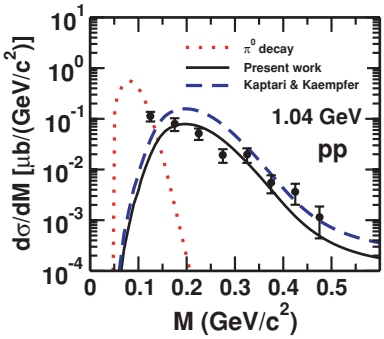

FIG. 4. (Color online) The calculated dilepton invariant mass distribution for the *pp* collision at the beam energy of 1.04 GeV in comparison to the DLS data. The contribution of the π^0 Dalitz decay is also shown here that is the same as that in Ref. [17].

elementary dilepton production cross sections. In the SPA model, the radiation from the internal lines [Fig. 1(c)] is neglected and the strong interaction vertex is assumed to be on-shell (which is reasonable only for small photon energies). This cross section is corrected by including a multiplicative factor that is the ratio of the phase space available to the two-nucleon system with or without the emission of a dilepton of invariant mass M [32].

It is desirable to check the reliability of the semiclassical calculations by comparing them with results of a full quantum mechanical model. In the upper panels of Fig. 5, we compare the invariant mass distributions of the *pn* bremsstrahlung cross sections obtained within the SPA and FQM approaches at the beam energies of 1.04 and 2.09 GeV. We note that the SPA (with corrected phase space) model results agree surprising well in shape with those of the FQM. This is, however, dependent on the values of the *np* total cross section used in the SPA calculations that is parameterized as $\sigma^{np}(s) = \alpha_1 m_N/(s - 4m_N^2) + \alpha_2$ mb (see, Ref. [32]), where $\alpha_1 = 18$ GeV mb and $\alpha_2 = 10$ mb and s is the square of the invariant mass in the incident channel.

In the middle panel of Fig. 5, we compare the DDD and FQM Δ isobar contributions to the dilepton spectra calculated within two models. We also show here the individual contributions of the postemission (dashed lines) and pre-emission (dotted lines) graphs to the FQM cross sections. We note that at both the beam energies pre-emission diagrams contribute substantially to the total FQM cross sections for $M > 0.3$ GeV. In the DDD model these diagrams are not included. In the lower panel of Fig. 5 we compare the total cross sections

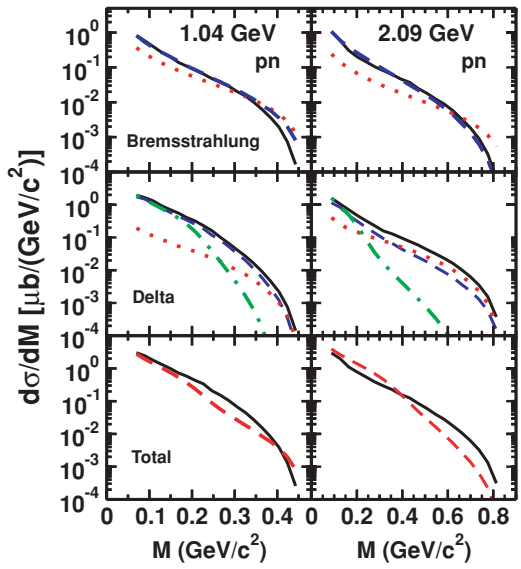

FIG. 5. (Color online) Comparisons of (i) the SPA and FQM *pn* bremsstrahlung contributions [SPA results with and without phase space correction are shown by dashed and dotted lines, respectively] (upper panel), (ii) the DDD (dashed-dotted lines) and FQM Δ isobar cross sections (middle panel); also shown here are the FQM postemission (dashed lines) and pre-emission (dotted lines) contributions, (iii) the sum of SPA and DDD contributions (dashed line) and the FQM total cross sections (lower panel). The FQM results are shown by solid lines.

obtained by adding the SPA and DDD contributions (termed as semiclassical) with those of the FQM. It is clear that for the important intermediate M values the two cross sections differ from each other noticeably. Therefore, care has to be taken in interpreting the transport model results obtained by using the semiclassical elementary dilepton production cross sections.

IV. SUMMARY AND CONCLUSIONS

In summary, we have presented a fully covariant and gauge invariant model for the dilepton production in elementary nucleon-nucleon collisions employing a pseudoscalar coupling at the nucleon-nucleon-pion vertex. With this coupling, the calculations do not involve the kind of gauge-invariance-related ambiguities that are present in those done with a pseudovector $NN\pi$ coupling.

We find that similar to the results of Ref. [17], our NN bremsstrahlung cross sections are lower than those of Ref. [16] by factors of 2–4 for dilepton invariant mass values below 0.6 GeV for both pp and pn collisions at 1.04 GeV as well as 2.09-GeV incident energies. However, the pp bremsstrahlung results of Ref. [18] where realistic T matrices have been used to describe the initial NN interaction are similar to those of our model at the beam energy of 2.09 GeV, while for 1.04-GeV incident energy they are larger (smaller) than our values for dilepton invariant masses smaller (larger) than 0.25 GeV. We stress, however, that the current arising from the nucleonic diagram in the model of Ref. [18] is not gauge invariant. An important point to note is that there is no overall multiplicative factor to differentiate our cross sections from those of Ref. [18]. It is expected that the results from the HADES group on the dilepton production in pp and pd collisions [30] would provide a fresh ground for differentiating between various models.

Calculations performed with a pseudovector $NN\pi$ coupling are more appealing because this coupling is consistent with the chiral symmetry requirement of the quantum chromodynamics [34] and also because it leads to negligible contributions from the negative energy states (pair suppression phenomena) [35]. However, in calculations with PV $NN\pi$ vertex the contact terms resulting from different prescriptions of restoring the gauge invariance will have to be carefully examined. This work is currently underway.

We found that the total dilepton production cross sections in the elementary NN collisions as calculated within the semiclassical models and used in most transport calculations differ noticeably from those predicted by the full quantum mechanical model. Therefore, quantum mechanical cross sections should be used as input in the transport model calculations of dilepton production in nucleus-nucleus collisions to interprete their results properly.

ACKNOWLEDGMENTS

We are grateful to Dr. G. Lykasov and Ingo Fröhlich for a careful reading of the manuscript and helpful comments. R.S. thanks A.W. Thomas for his very kind hospitality at the Theory Center of the Thomas Jefferson National Accelerator Facility where a part of this work was done. The Jefferson Science Associates operates the Thomas Jefferson National Accelerator Facility for the United States Department of Energy under contract DE-AC05-06OR23176.

[1] R. J. Porter *et al.*, Phys. Rev. Lett. **79**, 1229 (1997).
[2] G. Agakichiev *et al.*, Eur. Phys. J. C **41**, 475 (2005).
[3] D. Adamova *et al.*, Phys. Rev. Lett. **91**, 042301 (2003).
[4] R. Arnaldi *et al.*, Phys. Rev. Lett. **96**, 162302 (2006).
[5] S. Afanasiev *et al.*, arXiv:0706.3034 [nucl-ex].
[6] R. Rapp, J. Phys. G: Nucl. Part. Phys. **34**, S405 (2007); Nucl. Phys. **A782**, 275 (2007); H. van Hees and R. Rapp, Phys. Rev. Lett. **97**, 102301 (2006); J. Ruppert, C. Gale, T. Renk, P. Lichard, and J. I. Kapusta, *ibid.* **100**, 162301 (2008).
[7] C. Ernst, S. A. Bass, M. Belkacem, H. Stöcker, and W. Greiner, Phys. Rev. C **58**, 447 (1998).
[8] W. Cassing and E. L. Bratkovskaya, Phys. Rep. **308**, 65 (1999).
[9] R. Rapp and J. Wambach, Adv. Nucl. Phys. **25**, 1 (2000).
[10] K. Shekhter, C. Fuchs, A. Faessler, M. Krivoruchenko, and B. Martemyanov, Phys. Rev. C **68**, 014904 (2003).
[11] G. Agakichiev *et al.*, Phys. Rev. Lett. **98**, 052302 (2007).
[12] E. L. Bratkovskaya, W. Cassing, R. Rapp, and J. Wambach, Nucl. Phys. **A634**, 168 (1998).
[13] W. Cassing, E. L. Bratkovskaya, R. Rapp, and J. Wambach, Phys. Rev. C **57**, 916 (1998).
[14] G. Agakishiev *et al.*, Phys. Lett. **B663**, 43 (2008).
[15] E. L. Bratkovskaya and W. Cassing, Nucl. Phys. **A807**, 214 (2008).
[16] L. Kaptari and B. Kämpfer, Nucl. Phys. **A764**, 338 (2006).
[17] R. Shyam and U. Mosel, Phys. Rev. C **67**, 065202 (2003).
[18] F. de Jong and U. Mosel, Phys. Lett. **B379**, 45 (1996).
[19] K. Schmidt, E. Santini, S. Vogel, C. Sturm, M. Bleicher, and H. Stöcker, arXiv:0811.4073 [nucl-th].
[20] G. Penner and U. Mosel, Phys. Rev. C **66**, 055212 (2002); R. M. Davidson and R. Workman, *ibid.* **63**, 025210 (2001); H. Haberzettl, *ibid.* **56**, 2041 (1997); K. Ohta, *ibid.* **40**, 1335 (1989).
[21] A. Usov and O. Scholten, Phys. Rev. C **72**, 025205 (2005).
[22] M. Schäfer, H. C. Dönges, A. Engel, and U. Mosel, Nucl. Phys. **A575**, 429 (1994).
[23] P. C. Tiemeijer and J. A. Tjon, Phys. Rev. C **42**, 599 (1990).
[24] H. C. Dönges, M. Schäfer, and U. Mosel, Phys. Rev. C **51**, 950 (1995).
[25] K. Hagalin, J. Kapusta, and C. Gale, Phys. Lett. **B224**, 433 (1989).
[26] I. S. Towner, Phys. Rep. **155**, 263 (1987).
[27] T. Feuster and U. Mosel, Phys. Rev. C **59**, 460 (1999).
[28] M. Schäfer, T. S. Biro, W. Cassing, U. Mosel, H. Nifenecker, and J. A. Pinston, Z. Phys. A **339**, 391 (1991).
[29] F. de Jong and U. Mosel, Phys. Lett. **B392**, 273 (1997).
[30] I. Fröhlich *et al.*, arXiv:0712.1505 [nucl-ex].
[31] R. Rückl, Phys. Lett. **B64**, 39 (1976).
[32] C. Gale and J. Kapusta, Phys. Rev. C **35**, 2107 (1987); **40**, 2397 (1989).
[33] Gy. Wolf, G. Batko, W. Cassing, U. Mosel, K. Niita, and M. Schäfer, Nucl. Phys. **A517**, 615 (1990).
[34] S. Weinberg, Phys. Rev. **166**, 1568 (1968).
[35] R. Machleidt, K. Hollinde, and Ch. Elster, Phys. Rep. **149**, 1 (1987).